esa

ECOSPHERE

FRESHWATER ECOLOGY

# Homeostasis and non-linear shift in the stoichiometry of P-limited planktonic communities

Pau Giménez-Grau,[1] Marisol Felip,[2,3] Aitziber Zufiaurre,[2] Sergi Pla-Rabès,[2] Lluís Camarero,[4] and Jordi Catalan[2,5,†]

[1]*Department of Biology, Aarhus University, Aarhus C, Denmark*
[2]*CREAF, Cerdanyola del Vallès, Catalonia, Spain*
[3]*Departament de Biologia Evolutiva, Ecologia i Ciències Ambientals. Universitat de Barcelona, Barcelona, Catalonia, Spain*
[4]*Centre d'Estudis Avançats de Blanes (CEAB), CSIC, Blanes, Catalonia, Spain*
[5]*CSIC, Cerdanyola del Vallès, Catalonia, Spain*

**Citation:** Giménez-Grau, P., M. Felip, A. Zufiaurre, S. Pla-Rabès, L. Camarero, and J. Catalan. 2020. Homeostasis and non-linear shift in the stoichiometry of P-limited planktonic communities. Ecosphere 11(9):e03249. 10.1002/ecs2.3249

**Abstract.** Planktonic communities are naturally subjected to episodic nutrient enrichments that may stress or redress the imbalances in limiting nutrients. Human-enhanced atmospheric nitrogen deposition has caused profound N:P imbalance in many remote oligotrophic lakes in which phosphorus has largely become limiting. These lakes offer an opportunity to investigate the relationship between the changes in plankton stoichiometry, productivity, and community structure occurring during nutrient fluctuations in P-limited conditions. We performed P ($PO_4^{3-}$) and N ($NH_4^+$ or $NO_3^-$) pulse additions to the summer epilimnetic community of an ultraoligotrophic lake using self-filling ~100-L enclosures and analyzed the response to varying P availability, N:P imbalance, and N source. Seston C:N:P proportions remained fairly unchanged to P additions that were within the range of values seasonally found in the lake. However, the seston N:P ratio abruptly shifted and approached Redfield's proportions at P additions typical of mesotrophic conditions that provided non-limiting conditions. N surplus did not affect seston C:N:P proportions. The patterns of seston N:P stability and shift were similar for both N sources. In contrast, productivity was highly sensitive to low and medium P additions and decelerated at high P additions. Phytoplankton biomass dominated particulate organic matter. The autotrophic community differentiated almost linearly across the P gradient. Chrysophytes' dominance decreased, and diatoms and cryptophytes relative abundance increased. Nonetheless, the stoichiometry stability and non-linear shift involved large biomass proportions of the same species, which indicates that the bulk stoichiometry was related to similar physiological behavior of phylogenetically diverse organisms according to the biogeochemical context. The C:N:P seston stability in P-limited conditions—with loose coupling with productivity, nutrient supply ratios, and species dominance—and the sudden shift to Redfield proportions in P-repleted conditions suggest a complex regulation of P scarcity in planktonic communities that goes beyond immediate acclimation growth responses and might include alternative physiological and biogeochemical states.

**Key words:** ecological stoichiometry; ENEX experiment; experimental enclosures; mountain lakes; nutrient enrichments; oligotrophy; phytoplankton; seston.

**Received** 12 May 2020; accepted 20 May 2020; final version received 22 July 2020.. Corresponding Editor: Debra P. C. Peters.



† **E-mail:** j.catalan@creaf.uab.cat

## Introduction

The biomass of all living organisms consists of more than 20 essential elements in quite defined proportions, and whichever of these elements is in shortest supply than demand may be limiting the growth (Hessen et al. 2013). Demand for nitrogen (N) and phosphorus (P) is high in all organisms (e.g., synthesis of proteins and nucleic acids) and, indeed, typically limits productivity in many aquatic ecosystems (Elser et al. 2007). Human activities have not only increased the nutrient availability and productivity in lots of ecosystems, but also unbalanced natural N:P supplies and changed limiting conditions. At present, we still do not fully understand the links between stoichiometry, productivity, and species composition to evaluate the consequences of this fertilization and imbalance in planktonic communities. The elemental composition of phytoplankton and seston in aquatic ecosystems is less constrained to 106C:16N:1P than formerly thought (Geider and La Roche 2002, Sterner et al. 2008), although fast-growing phytoplankton presents a more rigid and P-rich elemental composition (Hillebrand et al. 2013). In P-limited conditions, strong negative relationships between growth and N:P have been suggested based on observations (Hillebrand et al. 2013) and model approaches that consider the protein: RNA ratio. In particular, the growth rate hypothesis (GRH) states that achieving high specific growth rates requires high concentrations of ribosomes, which are P-rich and increase the P content of organisms (Sterner and Elser 2002). According to the GRH, the N:P molar ratio of 16 (Redfield 1963) had been suggested to have no intrinsic optimality significance (Klausmeier et al. 2004*a*) and, quite the opposite, being the optimal stoichiometry in nutrient-replete conditions when the feedbacks between the protein and rRNA synthesis processes are considered (Loladze and Elser 2011). Experimental and field observations have provided mixed support to GRH, and other processes influencing the P cell quota also appear potentially relevant in defining cell C:N:P ratios (Moreno and Martiny 2018). Different stoichiometry states across the oceans also are fostering a system-wide view in which many unknowns remain concerning physiological and biogeochemical processes (Martiny et al. 2013).

Inputs of N and P into remote ecosystems through atmospheric deposition can be particularly unbalanced, as P—unlike N—has no gaseous phase and its presence in the atmosphere is necessarily associated with particles (e.g., dust, sea-salt, biogenic particles, combustion ashes; Mahowald et al. 2008). In general, non-dusty regions of Europe and North America show N:P depositional ratios several-fold higher than the Redfield ratio (Peñuelas et al. 2013, Wang et al. 2014), what is intensifying P limitation in aquatic ecosystems (Elser et al. 2009). The planktonic lake communities in these P-limited ecosystems are subjected to episodic P and N enrichments that modify for short periods (days to weeks) the P availability and the N:P imbalance. The way the communities respond to these fluctuations might provide some light to the stoichiometry regulation in P-limited conditions. However, nutrient fluctuations co-occur with temperature and light fluctuations throughout the lake's seasonal changes, which also may affect the plankton stoichiometry. Field experiments using nutrient additions within the range naturally occurring should help to disentangle nutrient supply effects on stoichiometry from other potentially confounding factors.

Consequently, the ENEX experiment in Lake Redon (Pyrenees) aimed to investigate the stoichiometry of P-limited planktonic communities using pulse nutrient additions on self-filling enclosures. The experiment was performed in the epilimnion, shortly after the onset of summer stratification, when the annual lowest nutrient concentrations in the lake water are found. The experiment consisted of phosphorus ($PO_4^{3-}$) and nitrogen ($NO_3^-$ or $NH_4^+$) additions to 20 m-long columnar enclosures to investigate a gradient of P enrichment and a gradient of N:P imbalance with alternative N sources. P and N additions were within the range of values seasonally found in the lake and other oligotrophic lakes of the Pyrenees, with further treatment with P levels typical of mesotrophic conditions that provided non-limiting conditions. Based on prevalent current views, the expected results were that (1) if cell stoichiometry and growth are tightly linked, the plankton (seston) N:P ratios would change coherently with productivity across the P enrichment gradient and should be close to Redfield ratio in non-limiting conditions; (2) if the N:P

supply ratio is similarly relevant to P supply quantities, changes should also occur across the N:P imbalance gradient with fix P availability; and, finally, (3) if protein synthesis plays a primary role in P-limited conditions, $NO_3^-$ or $NH_4^+$ supply could result in different productivity efficiency and stoichiometric ratios. These points could be summarized in an overall main expectation, that is, a high correlation between C:N:P ratios, productivity, and community composition across treatments. The results showed no such tight coupling between the three components of plankton response to nutrient treatments. There were non-linear relationships between them with a particularly stable stoichiometry in all P-limited conditions.

## Methods

### *Study site*

The ENEX experiment was performed in Lake Redon, an ultraoligotrophic high-mountain lake located in the Central Pyrenees (42°38′33″ N, 0°36′13″ E, 2232 m a.s.l). Lake Redon is quite sensitive to changes in atmospheric nutrient inputs such as the human-induced increase in N deposition, and the events of P enrichment caused by northern Africa dust deposition (Camarero and Catalan 2012). The lake is P-limited but shows marked seasonal changes in P, $NO_3^-$, and $NH_4^+$ availability (Ventura et al. 2000) due to seasonally changing external and internal loads during summer, and under-ice stratification periods, snowpack thawing and spring and fall water column overturns. The lake has been the center of intense limnological research for over 30 yr (Catalan et al. 2006). It is a dimictic lake with a surface area of 24 ha, and maximum and mean depths of 73 and 32 m, respectively (Catalan 1988). The lake is ice-covered about six months a year. During the ice-free period, the penetration of solar radiation is high, and the photic zone (40–50 m) extends beyond the seasonal thermocline (15–20 m). Phytoplankton is the main fraction of planktonic biomass and is usually dominated by chrysophytes (Felip et al. 1999). Other groups can be occasionally relevant during the mixing period (chlorophytes, diatoms), during summer stratification (dinoflagellates) or at greater depth (cryptophytes).

### *Enclosure features and manipulation*

In the ENEX experiment, we used self-filling enclosures that were built using tubular-shaped polythene bags (diameter 8.5 cm; length 20 m) and two polyvinyl chloride (PVC) tubes, attached one at each extreme of the bag (Fig. 1). The tube at the lower end was closed and served as a 0.5 m long sediment trap. The upper tube (1.5 m) enabled the gaseous exchange with the atmosphere. An expanded polystyrene float was attached to the upper tube to hold the enclosure at the water surface, and weight was tied at the sediment trap to stretch the bag. The enclosures were self-filled with ~100 L of water from 0 to 20 m lake depth, avoiding disturbances for the organisms. Once the enclosures were installed, we proceeded to specific enrichments. For each enclosure, a 20 m-long thin plastic tube was filled with 0.9 L of nutrient-enriched water, introduced inside the enclosure, and the solution was released homogeneously along the enclosure's water column as the tube was gently retrieved.

The enclosures were deployed on 5–6 August 2013 and recovered 25 d later. An integrated water sample (i.e., ~5 L, from 0 to 20 m deep) was obtained from each enclosure at the end of the experiment, using 20 m long plastic tubes pumping the water volume inside these tubes. The water sample was immediately filtered through a 250-μm pore size mesh to discard large zooplankton. There were three crustacean zooplankters in the lake. Two of them (*Diaptomus cyaneus* and *Daphnia pullicaria*) showed an avoidance reaction during filling, and they were absent or extremely low in the enclosures. The densities of *Cyclops abyssorum* did not decline respect to the water column, but the results did not show any significant correlation with the differences between enclosures. The sediment trap was collected just before removing the enclosure. The trap water content was decanted into a plastic bottle and kept until filtration in the laboratory. Once on land, water samples were filtered for dissolved nutrient analyses through precombusted (5 h, 450°C) glass fiber filters (GF/F, Whatman), and the material on the filters was used for particulate analyses. Samples were stored frozen until analyses in the laboratory. Between one and two liters of water were also filtered on glass fiber filters for chlorophyll *a* (Chl *a*) analyses, wrapped in aluminum foil, and

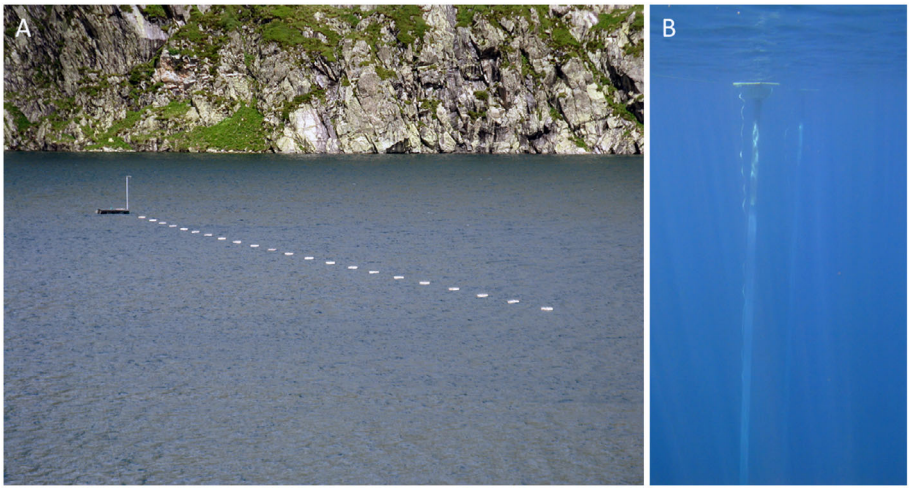


Fig. 1. (A) Enclosure deployment in Lake Redon. (B) Underwater view of the upper part of the enclosures.

frozen in liquid nitrogen to prevent degradation. Two subsamples were fixed to estimate microbial abundance: A 10 mL subsample was processed for prokaryotes following Medina-Sánchez et al. (2005), whereas a 200 mL subsample was preserved with 0.5% (vol/vol) alkaline Lugol's solution for protists (Sournia 1978). An integrated sample was collected on 6 August 2013 and processed as previously described to assess Chla and microbial abundance at the beginning of the experiment. Regarding the initial levels of C, N, and P in the dissolved and particulate fractions, we used samples collected on 8 August 2013.

### *Experimental design*

To assess the stoichiometry response to nutrient enrichment, we established one gradient of increasing P availability (P enrichment), and another gradient of increasing N availability (N:P imbalance; Fig. 2). Both P and N were added in all enriched treatments because the concentrations were initially relatively low for both nutrients, and the addition of only one nutrient could produce the other to become limiting. N and P were added in three different levels: low, intermediate, and high (Fig. 2A). The concentrations just after the nutrient addition of total dissolved phosphorus (TDP) and dissolved inorganic nitrogen (DIN) were estimated using the added mass of P and N, the water volume of the enclosures, and the initial concentrations of TDP and DIN in the lake (TDP, 0.022 µmol/L; DIN, 4.4 µmol/L). Thus, P additions resulted in rounded TDP initial concentrations of 0.06, 0.21, and 1.90 µmols/L, whereas N additions resulted in rounded DIN initial concentrations of 17, 35, and 73 µmol/L. The low P and N-enriched condition (N_P) emulated the initial DIN:TDP ratio (223:1) in the lake, but with higher concentrations (Fig 2B). From this N_P condition, the P enrichment was obtained maintaining the DIN level and increasing the P addition to medium (N_P+) and high levels (N_P++). Likewise, the N:P imbalance was obtained maintaining the low TDP level in N_P and increasing the N addition to medium (N+_P) and high levels (N++_P).

Initial lake DIN concentrations were dominated by nitrate ($NO_3^-$, 4.2 µmol/L; $NH_4^+$, 0.2 µmol/L). To determine the potential effects of varying $NH_4^+$:$NO_3^-$ supply on stoichiometry (N source effect), N was added as $NH_4Cl$ in five treatments and as $KNO_3$ in the other five. P was always added as $K_2HPO_4$. To specify which form of DIN was added, the treatment coding includes an H after the N when the form was $NH_4^+$ (NH++_P, NH+_P, NH_P, NH_P+, NH_P++) and an O when it was $NO_3^-$ (NO++_P, NO+_P, NO_P, NO_P+, NO_P++). A total of 22 enclosures were deployed. They included two replicates for each treatment, plus two non-enriched control enclosures. Unfortunately, we had technical incidences with some enclosures at different steps of the experiment. We lost one replicate of non-enriched, NO_P++,

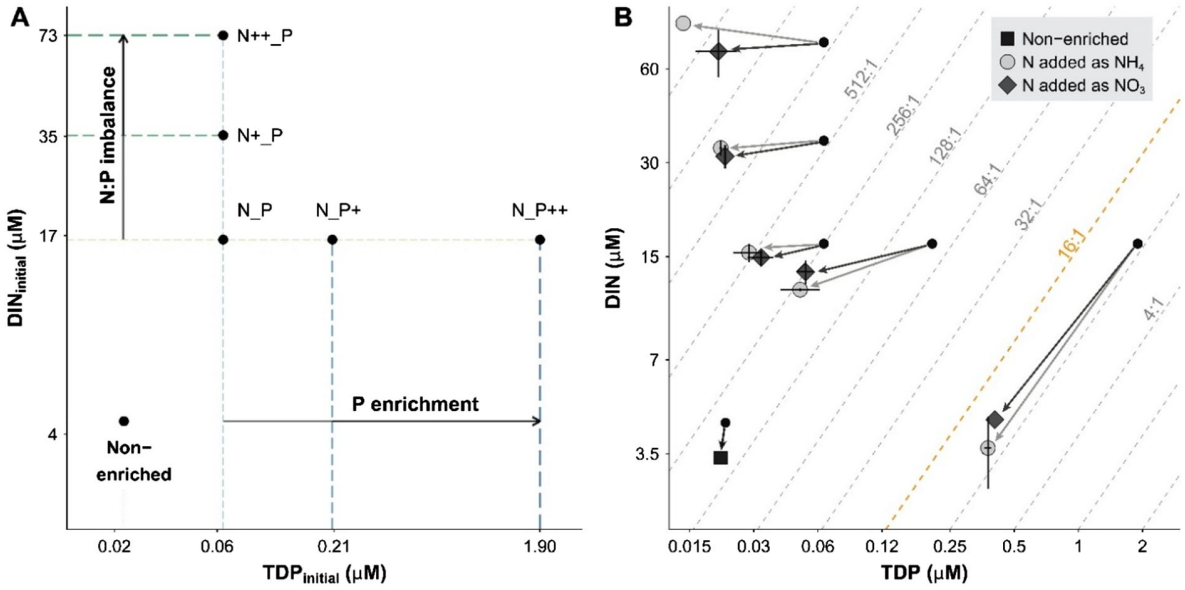


Fig. 2. (A) Experimental design indicating the initial DIN and TDP concentrations for each experimental condition and controls (black dots). The P-enrichment gradient and N:P imbalance are indicated. Note that treatment N_P belongs to both gradients. (B) Change of DIN and TDP concentrations from the beginning (black dot) to the end of the experiment for the respective treatments (squares, circles, and diamonds). Dashed lines indicate DIN: TDP molar ratios. Note that axes are in logarithmic scale.

and NH++_P treatments, respectively. Results are shown in the figures as dots for the average value of the treatment replicates and a line indicating the range (e.g., Fig. 2B). Treatment effects were evaluated using ANOVA and considering three factors (i.e., initial DIN and TDP levels and N source form). To avoid overpopulating the text with *P*-values, when we use the term significant in the results, it refers to *P*-values always lower than 0.03 and usually much lower. The experiment data can be accessed in the Dryad repository (Catalan et al. 2020).

### *Chemical analyses*

Total dissolved phosphorus (TDP) was determined by colorimetry using a segmented flow autoanalyzer (AA3HR, Seal/Bran + Luebbe) with an automated method based on Murphy and Riley's (1962) method (Bran + Luebbe method G-175-96), with samples previously digested by the acid persulphate oxidation (Grasshoff et al. 1983). $NH_4^+$ and $NO_2^-$ were determined by automated versions of the blue indophenol (Berthelot reaction) method (B + L G-171-96) and the Griess reaction (B + L G-173-96), respectively, and analyzed by colorimetry using the segmented flow autoanalyzer. $NO_3^-$ was measured by capillary electrophoresis (Quanta 4000, Waters). Dissolved inorganic nitrogen (DIN) was calculated as the sum of $NO_3^-$, $NO_2^-$, and $NH_4^+$. Dissolved organic carbon (DOC) was determined by catalytic combustion and infrared spectrometric detection of the $CO_2$ produced (TOC5000 Shimadzu analyzer). Particulate C and particulate N were determined using a Carlo Erba elemental analyzer. Filters for particulate P analyses were firstly digested using the acid persulphate wet oxidation, and the extracts analyzed by the same colorimetric method already specified for TDP. Stoichiometry ratios are expressed in molar terms throughout the text. Chla was firstly extracted in 5 mL 90% acetone with a sonication probe (Sonopuls GM70 Delft, The Netherlands; 50W, 2 min), and the extracts were subsequently centrifuged (4 min at 1006 x *g*, 4°C) and filtered through a Whatman Anodisc 25 (0.1 µm). Chla was analyzed by ultra-performance liquid chromatography (UPLC, Acquity, Waters, Milford, Massachusetts, USA), as reported in Buchaca et al. (2005).

*Plankton community, biomass, and productivity*

The abundance of eukaryotes was estimated using the Utermöhl method (Sournia 1978). Biovolume was determined by measuring the main cell dimensions and assimilating its shape to known geometric forms (Hillebrand et al. 1999). We estimated the changes in the autotrophic community composition as the Hellinger distance (Legendre and Gallagher 2001, Borcard et al. 2011, Oksanen et al. 2016) between each enriched enclosure and the non-enriched condition, using the biovolume of the major phylogenetic groups of autotrophs.

The abundance of prokaryotes was estimated as DAPI counts. Cells were filtered through 0.2 μm polycarbonate filters (Millipore, GTTP, 25 mm filter diameter), stained with DAPI (4′,6′-diamidino-2-phenylindole; 1μg/mL final concentration), and mounted on glass slides using Citifluor (Citifluor, UK). Slides were stored at −20°C in the dark until counting at the epifluorescence microscope at ×1000 magnification (>2000 cells per sample). We also examined the presence of autotrophic picoplankton at the epifluorescence microscope, but its abundance was negligible, in agreement with previous studies in Lake Redon (Felip et al. 1999).

The eukaryotic biovolume was transformed into carbon using a conversion factor of 0.2 pg C/μm$^3$ following Felip et al. (1999). Although this factor is size-dependent, we keep it constant because the range of size was small compared to other systems (Mullin et al. 1966, Menden-Deuer and Lessard 2000). According to their mean biovolume (0.051 μm$^3$), and the allometric equation proposed by Norland (1993), we transformed the abundance of prokaryotic cells to C biomass using a conversion factor of 0.014 pg C/cell. The sum of prokaryotes and eukaryotes will be referred to as "cellular particulate C" ($C_{cell}$). Because the system can be assumed as closed for dissolved and particulate organic carbon, net primary production (NetPP) was estimated by the balance between the final and the initial total organic carbon in the enclosures, including dissolved and particulate fractions.

At the end of the experiment, we checked the bags' surface microscopically. Only in the highest P enrichments, there were some localized spots of *Spirogyra* (filamentous chlorophyte). Bacterial biofilms cannot be discarded across treatments. Nevertheless, the nutrient levels in the enclosures remained high during the experiment; therefore, the potential wall activity could not have modified the planktonic growth conditions significantly.

## Results

*Productivity and C export*

Net primary production (NetPP) increased significantly with P enrichment (Fig. 3). Particulate C mainly determined the NetPP patterns, with significant differences between N supply forms, increasing up to ~3.7× with $NH_4^+$, and ~2.8× with $NO_3^-$ in the highest P additions (Fig. 3B). Nonetheless, DOC increase constituted a substantial fraction of the NetPP (~40–90%), with a similar absolute amount at all P levels (Fig. 3C). The NetPP response to P enrichment tended to decelerate at high P levels (note the logarithmic scales in Fig. 3); the relative increase was higher in N_P+ than in N_P++ treatments.

In contrast to P enrichment, NetPP barely changed across the N:P imbalance gradient (Fig. 3A). The DOC contribution to NetPP was about twice the particulate contribution (Fig. 3B).

Between 3% and 13% of NetPP was exported to sediment traps during the experiment. The percentage of exported C was lower in the more productive conditions (6–8% at N_P+, and 3–4% at N_P++). Although NetPP significantly increased at N_P+ and N_P++, the amount of particulate C accumulated in the sediment traps did not (Fig. 3D).

*Seston components*

The biomass of autotrophs was always higher than that of heterotrophs (prokaryotes plus eukaryotes). The percentage of autotrophs to all microorganisms ranged from 55% up to 88%. Initially, this percentage was 66% and only slightly declined under non-enriched conditions (62%). Lower percentages were observed at N:P imbalanced conditions (N++_$P_{mean}$ = 59%; N+ _$P_{mean}$ = 64%) than at the rest of treatments (N_$P_{mean}$ = 79%; N_P+$_{mean}$ = 86%; N_P++$_{mean}$ = 81%). The high contribution of autotrophs to cellular particulate C was reflected in nearly identical patterns to P enrichment and N:P imbalance (Fig. 4A,E).

The biovolume of autotrophs highly correlated with Chla ($n = 19$, $P < 0.0001$, $R^2 = 0.95$) and NetPP ($n = 19$, $P < 0.0001$, $R^2 = 0.91$) showing

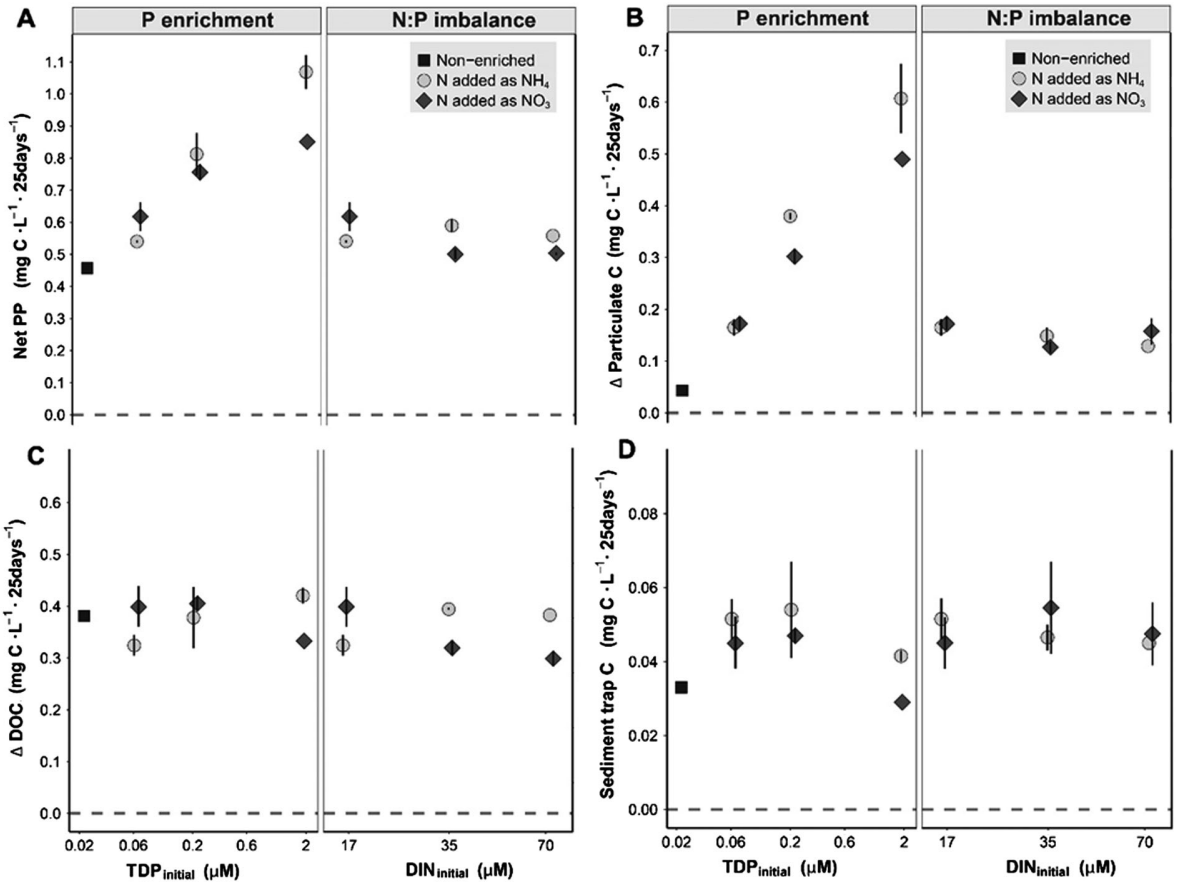


Fig. 3. Effects of P enrichments and N:P imbalance on Net Primary Production (A), water column particulate carbon change (B), DOC change (C), and sediment trap particulate carbon flux (D). For comparison between panels, data are provided in changes of homogenized concentrations throughout the 100 L of the enclosure during the 25 d of the experiment.

similar patterns of response to P enrichment: a steep increase at medium P additions and a decelerated increase at high (Fig. 4A,B). The increase of autotrophs at high P additions was also significantly more intense with $NH_4^+$ (~4.3×) than with $NO_3^-$ (~2.1×) dominance.

The autotrophic biovolume achieved in the N:P imbalance treatments was similar to those initially present in the lake and the non-enriched enclosures. The patterns of response differed slightly from those of NetPP. There was a significant negative effect of the N:P imbalance in the autotrophs' biovolume (Fig. 4A).

The pattern of eukaryotic heterotrophs resembled that of autotrophs. The biovolume of eukaryotic heterotrophs declined in non-enriched and low P-enriched, and N:P imbalance treatments compared to initial values (Fig. 4C). However, high P additions significantly increased this biovolume (2–5×).

The patterns of prokaryotes showed some differences from that of eukaryotes (Fig. 4D). Prokaryotic abundance increased in all experimental conditions, and the enhanced N:P imbalance did not negatively affect their abundance. The prokaryote response to high P additions was significantly much higher than to medium P additions. $NO_3^-$-rich treatments were significantly higher than the $NH_4^+$ at the highest P additions.

The amount of extracellular particulate C—assessed as the difference between particulate C

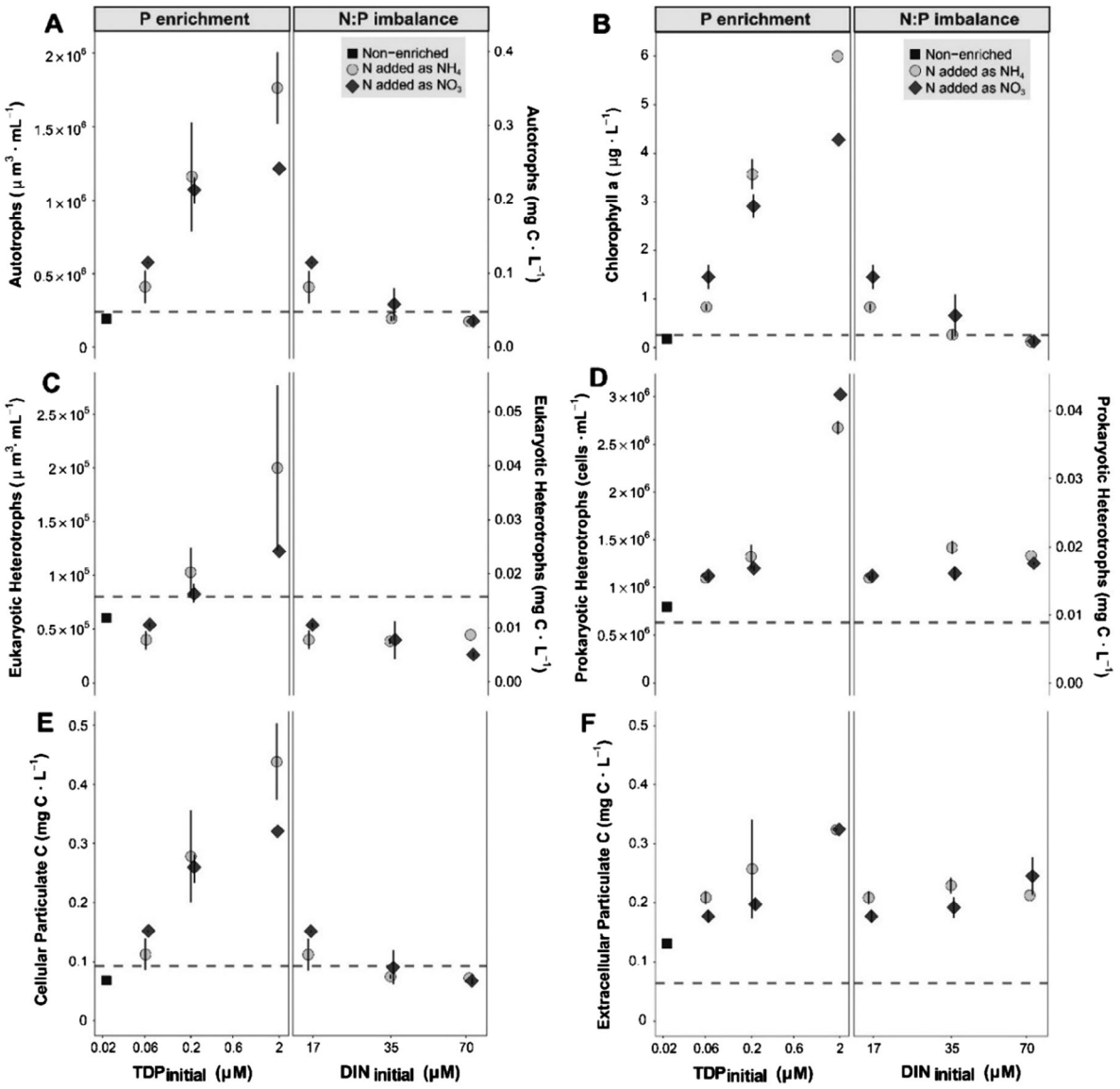


Fig. 4. Effects of P enrichment and N:P imbalance on different seston components: autotrophs (A), eukaryotic heterotrophs (C), prokaryotic heterotrophs (D), cellular particulate C (E), and extracellular particulate C (F). In (B), chlorophyll *a* levels are shown for comparison with the autotrophic biovolume. In (A) and (C), left *Y*-axes show biovolume units, whereas right *Y*-axes show biomass units. In (D), the left *Y*-axis shows abundance units, whereas the right *Y*-axis shows biomass units. Dashed lines indicate initial lake levels.

and cellular particulate C—was less variable than the cellular fraction (Fig. 4F) and ranged from 33% to 82% of total particulate C. The initial 41% increased up to 66% under non-enriched conditions. The extracellular fraction was proportionally higher at N:P imbalanced than P-enriched conditions ($N{+}{+}\_P_{mean} = 77\%$; $N{+}\_P_{mean} = 72\%$; $N\_P_{mean} = 60\%$; $N\_P{+}_{mean} = 46\%$; $N\_P{+}{+}_{mean} = 45\%$). Microscope observations showed that debris of dead organisms, prokaryotes, and also eukaryotes were often found within mucilaginous lumps and aggregates. In absolute terms, higher amounts of extracellular particulate were detected at the most P-enriched conditions,

where the visual detection of mucilaginous aggregates also increased.

### *Structure of the autotrophic community*

Both P enrichment and N:P imbalance treatments differentiated the autotrophic community respect to the non-enriched enclosure, though the effects produced by P enrichment were significantly stronger (Fig. 5A). Also, the differentiation was significantly higher with $NH_4^+$ addition. The abundance of chrysophyceae was a primary driver of changes in the autotrophic community since it was the dominant phytoplankton group (Fig. 5B). The relative abundance of chrysophyceae reached maximum values at N_P (61–71%) and declined with increasing P and N availability. Cryptophyta and Bacillariophyta became relevant groups and co-dominated the autotrophic community at the most P-enriched conditions. In the case of Bacillariophyta, the growth was significantly more intense with $NH_4^+$ than with $NO_3^-$. Bacillariophyta also became relevant in relative terms in the most N:P imbalanced enclosures as they did not decline in absolute terms as chrysophyceae.

There were a few species with a substantially higher contribution to the biomass of the planktonic community in each treatment (Fig. 6). However, one of these species rarely contributed more than 25% of the total biomass, and the few more abundant rarely more than 50% (Appendix S1: Fig. S1). Thus, a wealth of the biomass was generally the result of small contributions by many species. In fact, two of the dominant taxa (i.e., *Chromulina* spp [5 μm] and *Ochromonas* spp [7 μm]) were combinations of several species by their size. The diatom *Fragilaria nanana* was the single species with higher contribution to biovolume (Fig. 6), specifically, in the P+ and P++ treatments but also in NO++_P treatments (Appendix S1: Fig. S1).

### *C to N and P ratios*

Seston C:N ratio declined in all experimental conditions respect to the initial 9.6C:1N (Fig. 7A). Seston C:N was highly constant at the end of the experiment, ranging from 8.1 up to 8.9, with the only exception of the most P-enriched condition, which ratios were significantly lower (6.1–6.4). Conversely, seston C:P tended to increase in most experimental conditions respect to the initial

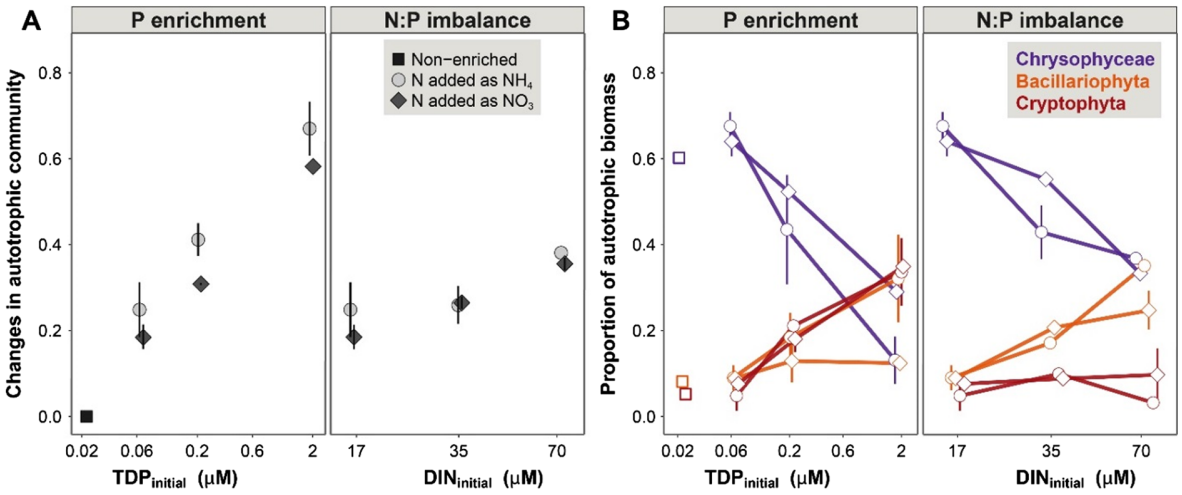


Fig. 5. Effects of P enrichment and N:P imbalance on the structure of the autotrophic community. (A) The Hellinger distance of autotrophic community in each treatment respect to the non-enriched treatments. (B) Changes in the biomass proportion of the main phytoplankton groups: Chrysophyceae (purple), Bacillariophyceae (orange), and Cryptophyta (red). The sum of these three groups represented 66% up to 91% of total autotrophic biomass. Squares, circles, and diamonds stand for non-enriched, $NH_4^+$-enriched, and $NO_3^-$-enriched conditions, respectively.

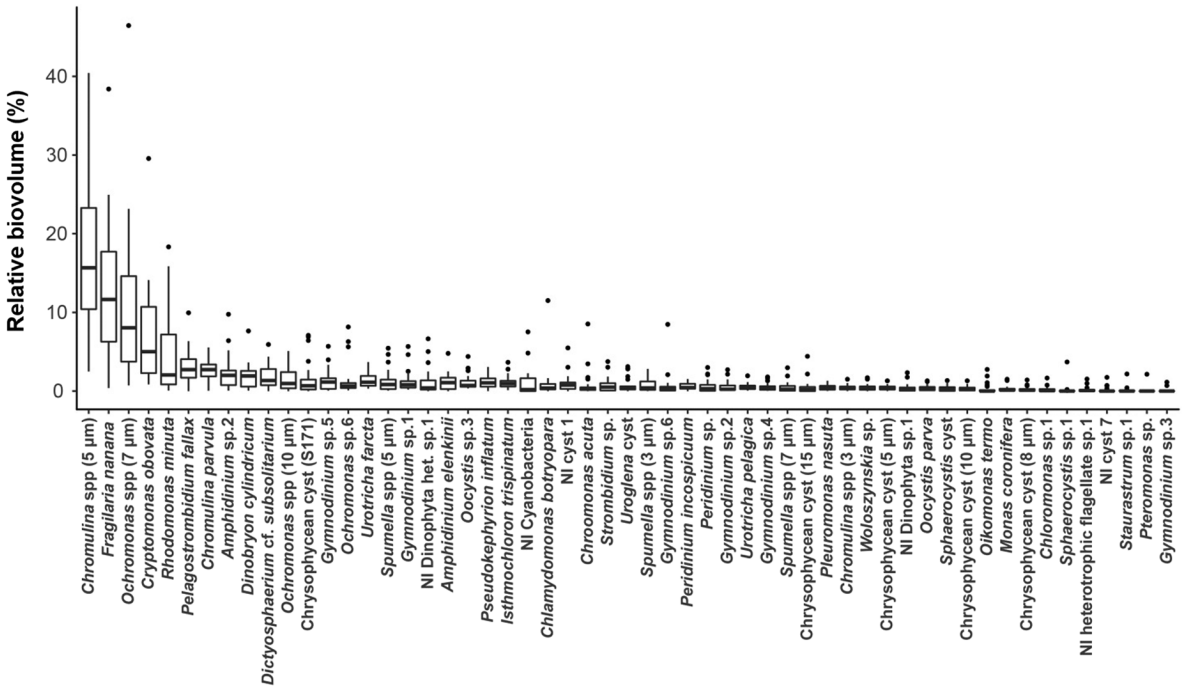


Fig. 6. Distribution of the relative biovolume of the main taxa found in the ENEX experiment ranked by their mean contribution. Box-plots indicate the median (crossbar), the 25 and 75 interquartile range (box), and 1.5× this interquartile range (whiskers). NI, non-identified.

value of 285 (Fig. 7B) and typically ranged from 280 to 520. However, the most P-enriched conditions showed seston C:P ratios significantly lower (80–110).

The C to N and P ratios calculated using the cellular particulate C ($C_{cell}$) instead of total particulate C should indicate a lower limit estimation of the cell stoichiometry ratios as it assumes that there is no extracellular particulate N and P. $C_{cell}$:N ranged from 1.5 to 5.6, and $C_{cell}$:P from 40 to 260 (Fig. 7A,B). These ratios were markedly lower than the corresponding seston ratios. In any case, both $C_{cell}$:N and $C_{cell}$:P were too low for cellular material, suggesting that the assumption of no extracellular particulate presence of N and P was wrong and thus that seston ratios were likely indicative of the dominant cell stoichiometry.

Particulate matter exported to sediment traps was N-impoverished under non-enriched conditions (C:N = 12.3) respect to the initial and final seston ratios (Fig. 7C). As observed for seston, the C:N ratio of the sediment trap matter significantly declined at high P additions. $NO_3^-$:P imbalance did not affect the C:N of the sediment trap matter, but the $NH_4^+$:P treatments showed significantly slightly lower C:N ratios. The sediment trap matter was more P-rich (or more C-poor) than seston at N_P and N_P+ conditions (Fig. 7D), but the differences between sediment and seston were considerably smaller at N_P++.

### *N:P stoichiometry*

Contrasting DIN:TDP conditions among treatments were maintained until the end of the experiment despite the likely progressive uptake during the execution. The concentrations of DIN and TDP in the enclosures remained almost unchanged under non-enriched conditions during the experiment (Fig. 2B). TDP concentrations declined markedly at low and medium P additions, and the decline of DIN was proportionately small. Consequently, DIN:TDP increased markedly at the end of the experiment in these treatments. Net assimilation of TDP increased when DIN availability was higher (N:P imbalance). At high P additions, TDP fell even more

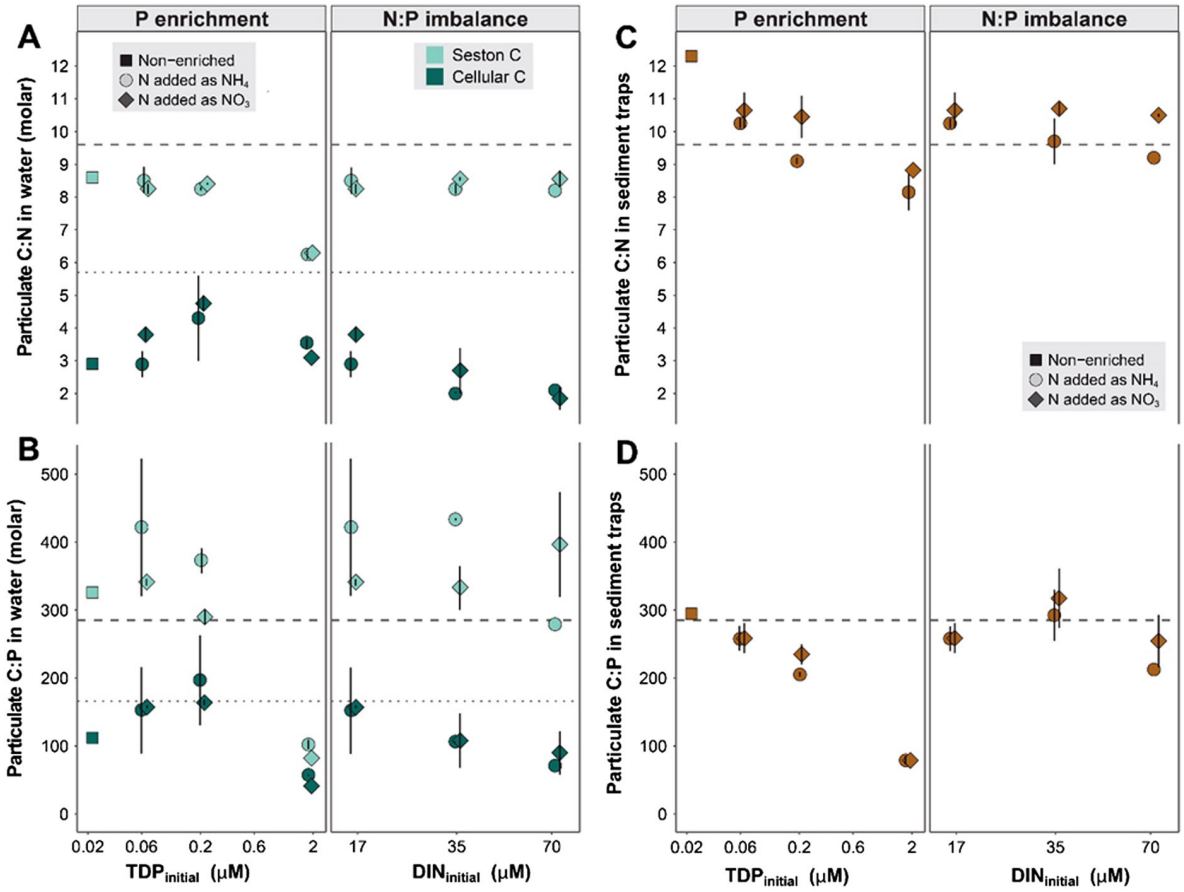


Fig. 7. Effects of P enrichment and N:P imbalance on C:N and C:P ratios of water column particulate matter (A, B) and sediment trap particulate matter (C, D). In (A) and (B), C:nutrient ratios were calculated using the total particulate (C) (light blue) and the cellular particulate C (dark blue). Dashed and dotted lines indicate initial lake ratios of total particulate C and cellular particulate C, respectively.

sharply, but DIN also declined importantly, and DIN:TDP ratios barely changed (~10:1).

The stoichiometry of seston did not mirror the N:P proportions in the supply nutrients. In most treatments, seston N:P increased from an initial value of ~30 to a range between ~33–65. Nonetheless, noteworthy, N:P significantly declined at N_P++ to Redfield proportions (~13–17) (Fig. 8A). Seston from non-enriched and NO_P treatments—which had similar initial DIN:TDP but different absolute concentrations of DIN and TDP—showed no significant differences. As observed for seston C:P, seston N:P tended to be higher when $NH_4^+$ was the dominant form of DIN, although variation was high and overall not significant.

In the sediment traps, the general pattern of N:P ratios was similar to that in seston but with a shift to lower values (Fig. 8B)— ~20–35 in most treatments and ~9–10 in N_P++—and without differences between treatments of distinct forms of N supply (Fig. 8B).

## Discussion

### *Seston stoichiometric stability under P limitation*

In the experiment, seston C:N:P was rather stable (~340C:40N:1) at P levels within the typical annual lake range but shifted drastically and approached the Redfield ratio (106C:16N:1P) when mesotrophic levels of P ($TDP_{initial}$ ~ 2µmol/L) were added. Although in this latter situation, the

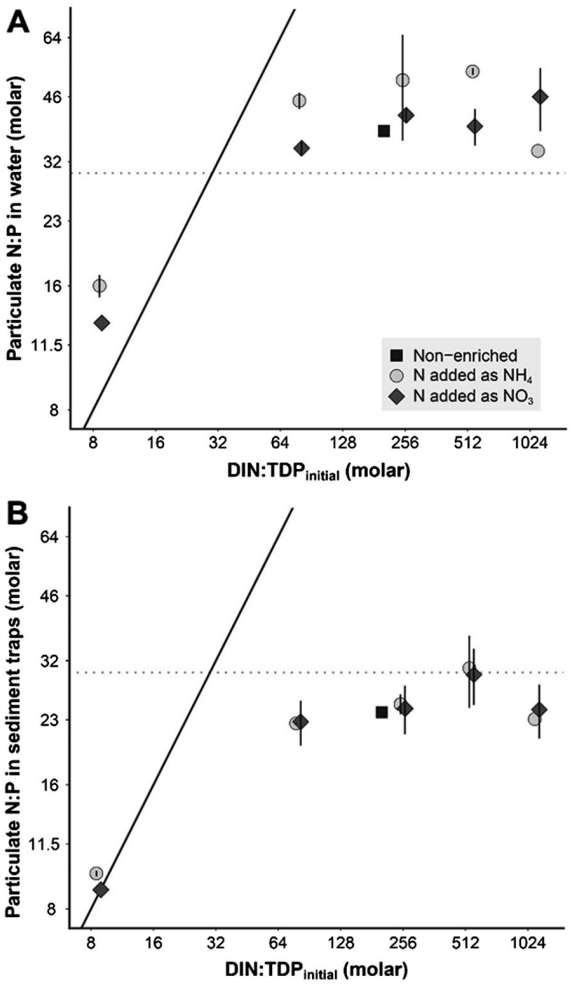


Fig. 8. N:P stoichiometry of seston (A) and sediment trap matter (B). Strict stoichiometric flexibility is accomplished when N:P of consumers reflects N:P of supplies, following the same slope that the solid black line. In contrast, strict homeostasis appears when N:P of consumers stays constant, independently of supply (a horizontal line). The horizontal dotted line indicates the seston N:P ratio at the beginning of the experiment.

source DIN:TDP ratio was slightly below the Redfield ratio, the absolute levels of P and N were so high compared with the potential demand by the plankton biomass that growth could be considered to occur in N- and P-repleted conditions. In all treatments within the P-limitation range, the seston stoichiometry was resistant to changes in absolute and relative P availability. The comparison of non-enriched and NO_P treatments is particularly illustrative. At the beginning of the experiment, these treatments had similar DIN:TDP ratio (256:1) but different concentrations of DIN and TDP. Considering the P deficiency of the lake, we could expect that seston of the NO_P treatment would become P-richer than the seston of the non-enriched treatment if seston stoichiometry were driven by the nutrient supply ratio (Klausmeier et al. 2004*a*). However, this was not the case, the seston N:P ratio barely changed. Nonetheless, productivity was considerably higher at NO_P than at non-enriched conditions. In fact, the increase in productivity between non-enriched and NO_P conditions had a similar rate of change than between NO_P and NO_P+ (Fig. 9), indicating that such increase was driven by the addition of P rather than a co-effect of P and N. Therefore, there was no hard dependence between the stoichiometry ratio and productivity in P-limited conditions.

High DIN additions (i.e., >17μM $DIN_{initial}$; >256:1 molar $DIN:TDP_{initial}$) did not produce any significant effect on seston N:P. In a recent meta-analysis of seston stoichiometry, more than 90% of N:P ratios placed below ~60 (Sterner et al. 2008). In Lake Redon, seston N:P beyond ~60 also appears unlikely, regarding the maximum values annually detected in this lake (Ventura and Catalan 2005). Some constraints may prevent higher seston N:P imbalances, such as the minimum P quotas and maximum N storage capacity of organisms (Hall et al. 2005). N excess availability did not lower seston C:N either. Indeed, seston C:N:P was remarkably insensitive to varying DIN and TDP levels above ~64DIN:1TDP. Wider ranges for seston C:N:P in Lake Redon along the year have been reported (Ventura and Catalan 2005), suggesting that other factors (e.g., light, temperature) may also affect seston C:N:P throughout the year (Hessen et al. 2013).

The extracellular particulate material can influence seston C:N:P proportions. In Lake Redon, DOC is highly correlated with particulate C, probably through a link with the extracellular—or detrital—fraction (Camarero et al. 1999). Prokaryotic abundance and extracellular particulate showed similar response patterns to experimental treatments (Fig. 4), which suggests that the presence of the mucilaginous aggregates

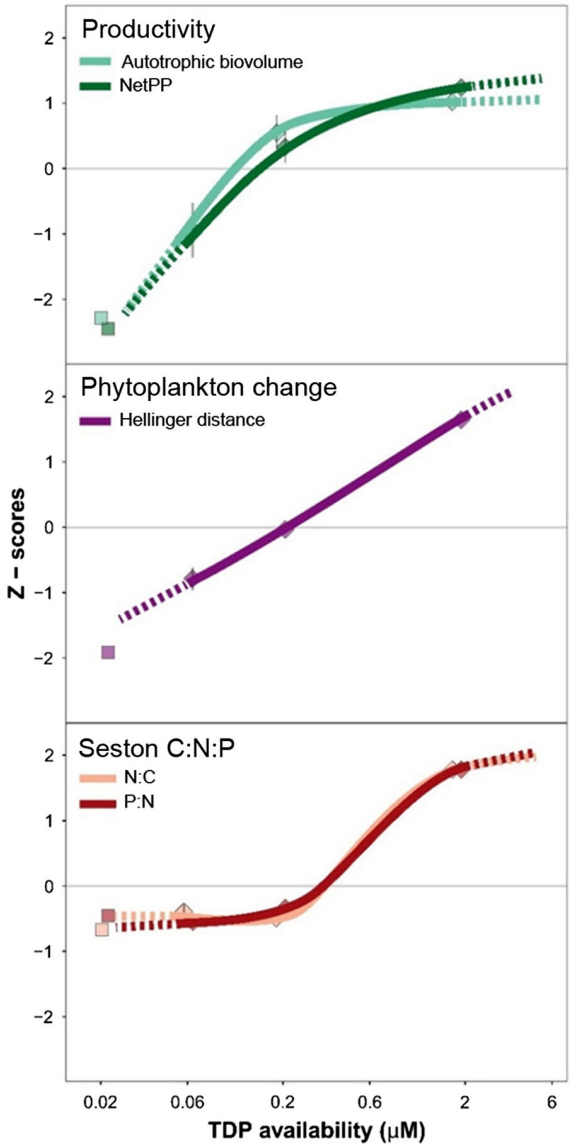


Fig. 9. Comparison of patterns of productivity, autotrophic community (phytoplankton) change, and seston C:N:P across the P-enrichment gradient. Note that the elemental composition of seston is shown as N:C and P:N ratios (instead of C:N and N:P ratios) to easily compare the patterns of change in productivity and community structure. Only $NO_3^-$-dominated conditions are shown for simplicity. Original values were standardized using the mean and standard deviation of NO_P, NO_P+, and NO_P++ enclosures. $NH_4^+$-dominated treatments provide similar results. Solid lines indicate the tendency within the study range, whereas dashed lines extend that tendency to lower and higher P availability. The non-enriched condition (squares) had lower DIN concentrations initially than the other conditions (diamonds), and, consequently, it is only shown as a reference.

(Fig. 9. *Continued*)

could favor prokaryotes, or, as occurs in marine snow, actively contribute to their formation (Azam and Malfatti 2007). C compounds did not exclusively constitute the extracellular matter. The $C_{cell}$:N and $C_{cell}$:P were unrealistically low when assuming that no N or P was present in the extracellular material. Thus, it does not seem that extracellular material played any significant role in seston C:N:P variation. The extracellular carbon regularly increased in both P enrichment and N:P imbalance gradients.

### *Seston stoichiometric driven by phytoplankton*

Seston is a mixture of autotrophs, heterotrophs, and detritus that can hardly be separated. Changes in nutrient availability and productivity may affect the proportion of the different seston fractions. Since autotrophs are frequently the dominant fraction, and the major contributors to detritus, the C:N:P composition of seston is commonly assigned to primary producers. Also, C:N:P composition of heterotrophic organisms tends to be more homeostatic than the autotrophic (Persson et al. 2010). Major algal groups present distinguishable C:N:P compositions (Quigg et al. 2003), and, therefore, changes in the phytoplankton community could also directly affect the seston C:N:P proportions. In our experiment, as the living matter was dominated by autotrophs (~80%), we expected that changes in the autotrophic community should have a dominant effect on seston composition. Indeed, neither the proportion of cellular to total particulate matter nor the proportion of autotrophic to total living biomass changed substantially between the N_P+ and N_P++ treatments. In contrast, the increase of prokaryotic abundance between these treatments was substantial (i.e., 5–8% in N_P+ and 10–14% in N_P++), but prokaryotes only represented a small fraction of the living biomass and, hence, cannot account for the seston stoichiometric changes. Therefore, phytoplankton appears as the driver of the stoichiometry

stability in the variety of P-limited conditions and the non-linear change in P-repleted conditions. We may wonder whether these patterns were due to a dominance of some particular species or related to a rather general change in cell stoichiometry across the community.

Chrysophyceans were the dominant phytoplankton group and mostly responsible for the observed pattern. The highest chrysophycean biovolume was found at medium P additions, and their relative contribution diminished progressively from N_P to N_P++ conditions (Fig. 5), in favor of diatoms and cryptophytes. Actually, the differentiation of the autotrophic community composition took place almost linearly with P addition and followed a different pattern than those observed for productivity and stoichiometry (Fig. 9). The relative abundance of chrysophyceans, diatoms, and cryptophytes already changed at N_P+ compared to N_P, while the change of seston C:N:P between these treatments was small. Moreover, if chrysophyceans had higher N:P ratios than diatoms and cryptophytes, we would have expected higher seston N:P at NO_P++ (where they represented ~29% of autotrophic biomass) than at NH_P++ conditions (~14% of autotrophic biomass), but the opposite was the case. Usually, diatoms show lower N:P ratios than the rest of phytoplankton groups (Quigg et al. 2003, Weber and Deutsch 2010), although the variation between phylogenetically close species is considerable. Diatoms increased their relevance in N_P++ treatments, but their contribution to biomass was always lower than 30%. Furthermore, although a few species in each treatment generally dominated phytoplankton biomass, these species differed depending on the treatment. Also, there were cases in which the same species was largely dominant in samples of contrasting seston N:P ratios (e.g., *Fragilaria nanana* in NH_P++ and NO++_P treatments). Therefore, all evidence point that the stoichiometric shift was not driven by the change in species dominance but, preferably, by the change of the C:N:P cell composition of many organisms.

### *Phytoplankton stoichiometry homeostasis in P-limited conditions*

Accepting that the observed seston stoichiometry changes in our experiment were mainly driven by phytoplankton, our results indicate C:N:P homeostasis in the range of P limitation naturally occurring in the lake. Although productivity was increasing with higher P availability, the stoichiometry ratios did not change. It seems that alternative growth rates could be achieved with a similar P cell quota within P limitation. The C:N:P ratios shifted to Redfield proportions when P additions provided nutrient-repleted conditions. Early chemostat experiments with single species had shown non-linear relationships between growth rate, and internal and external nutrient concentrations: slow growth cells showing lower minimum P quota than fast growth cells, with a threshold transition between the two states (Droop 1974).

The elemental composition of autotrophs depends on the relative abundance of structural macromolecules and nutrient stores (Rhee 1978, Elrifi and Turpin 1985). Ribosomes have received much attention because they may be a relevant pool of P in organisms (Geider and La Roche 2002) and are related to the growth capacity of organisms (Sterner and Elser 2002). In our experiment, seston C:N:P ratios achieved Redfield proportions in treatments released from P deficiency. According to the latest GRH formulations (Loladze and Elser 2011), the mutual feedback between protein synthesis and rRNA synthesis will result in a stable protein:rRNA mass ratio of $3 \pm 0.7$, which corresponds to an N:P Redfield ratio, under nutrient-repleted conditions. In that sense, results agree with expectations.

Ribosomes also provide an explanation for declining of phytoplankton N:P ratios at increasing growth rates (Goldman et al. 1979, Hillebrand et al. 2013). Some theoretical models predict non-linear and drastic transitions from the optimal N:P states at N- and P-limited conditions, toward the optimal N:P state at exponential growth conditions (Klausmeier et al. 2004*b*). However, these models expect a connection between the nutrient supply ratios and the cell N:P ratios within P-limited conditions, which did not correspond with our observations. In our experiment, productivity and seston N:P were clearly decoupled (Fig. 9), and stoichiometry was stable within P limitation at different growths and nutrient supply ratios.

The growth rate hypothesis has been questioned (Flynn et al. 2010) because it does not

consider P accumulation in non-ribosomic pools that could underlie stoichiometry relationships with growth (Hillebrand et al. 2013). For instance, phytoplankton can use non-phosphorus membrane lipids under P deficiency but increase phospholipid synthesis when it is more available (Van Mooy et al. 2009). Besides, a considerable amount of P can be adsorbed at the cellular surface of phytoplankton (Sañudo-Wilhelmy et al. 2004, Fu et al. 2005), which may directly link P availability in the medium and the P content of organisms. All these processes would affect the N:P ratio. If ribosome-P were only a minor component of the P quota, the association between C:P or N:P and growth rate under P limitation would not be necessary.

In our experiment, seston C:N also declined substantially at high P additions, and, therefore, the stoichiometric shift was not only related to a change of P content but points to the general regulation of the cell stoichiometry, including proteins. Nutrient limitation effects on all N and P cell pools, including storage, and their regulation still require much investigation.

### *Nitrogen effects on P-limited conditions*

The increase of N excess in the treatments resulted in a decline of total phytoplankton biomass, and the alteration of the community structure (Figs. 4A–B, 5A–B). This N negative effect offset the potential positive effect of the low amounts of P added as well. A possible increase in grazing should be discarded since the abundance of eukaryotic heterotrophs also declined. More likely, high DIN concentrations could be toxic for some phytoplankton species. The decline of autotrophic biomass was not paralleled by a similar reduction of particulate C, due to slight increases of prokaryotic and extracellular C. These latter planktonic compartments are expected to respond to the presence of dead organisms. Lower TDP levels at the end of the experiment under high N:P imbalanced conditions—but higher DIN than initially (Fig. 2B)—might be regarded as a consequence of the increased prokaryotic decomposing activity. Nonetheless, the seston N:P ratio did not change beyond the range observed in the P enrichments.

Accumulation of dead organisms and their decomposition can also influence seston C:N:P proportions. Under non-enriched conditions, sediment trap matter was markedly N-impoverished compared to the initial and final seston C:N:P composition in the water column. This feature indicated that mineralization of particulate N was higher than that of C and P. Indeed, the C:P of the sediment trap matter placed between the initial and final seston C:P, showing that mineralization of both elements was similar. The low mineralization of P in comparison with N (or even C) has been previously described for lakes (Elser and Foster 1998). Some P-containing molecules and aggregates (e.g., polyphosphates) can be difficult to mineralize in the water column (Diaz et al. 2008) and thus contribute to P deficiency in the ecosystem. Absolute C sedimentation did not substantially vary among experimental conditions, and, hence, the percentage of C in the sediment traps to NetPP declined as P availability, and productivity increased (from ~10% up to ~3% at N_P++). Lower mortality of organisms and enhanced mineralization of organic matter under P-enriched conditions may drive that tendency. Indeed, C:P and C:N ratios in the sediment traps linearly declined with increased P enrichment, whereas they were quite stable and similar to the initial matter in the N:P imbalance treatments. P shortage seems to enhance nutrient recycling from decaying organisms.

## Conclusions

The C:N:P seston stability in P-limited conditions found in our experiment—with loose coupling with productivity, nutrient supply ratios and species dominance—and the sudden shift to Redfield proportions in P-repleted conditions suggest a complex regulation of P scarcity in planktonic communities, which may go beyond immediate acclimation growth responses and might include alternative physiological and biogeochemical states.

Although P quotas have been suggested to be more sensitive to nutrient limitation (Moore et al. 2013) and thus C:P and N:P ratios may show more variation than C:N, our results suggest a linked regulation of N and P quotas. Performing similar experiments in N-limited systems (Warner et al. 2017) should improve the perspective of cell stoichiometry regulation in nutrient-limiting conditions. Rather than limited to elemental

measurements, experiments will benefit from assessing different P and N pools and indicators of growth regulation. For instance, direct measurements of ribosome content at the single-cell level (Biswas et al. 2019) would be useful to investigate whether the homeostasis is shared by most of the species in the community or restricted to some dominant subset.

The observed enhanced recycling of decaying organisms in P-limited conditions also indicates that stoichiometry stability may include interactions in biogeochemical processes in addition to physiological cell regulation (Moreno and Martiny 2018). We may ask if some regulation at the community level emerges from individual homeostasis and interactions between autotrophs and eukaryotic and prokaryotic heterotrophs. We may conjecture that the seston stability observed at P limitation and the non-linear shift in P-repleted conditions could be attributed to alternative states in the stoichiometry organization of the planktonic microbial community. If such states do exist, experiments submitting the community to back and forth shift between P-limited and P-repleted conditions will allow identifying a range of P availability in which the system will show hysteresis in the transition between the two hypothetical alternative states.

## Acknowledgments

The research was funded by research grants of the Spanish Government NitroPir (CGL2010–19737) and Transfer (CGL2016–80124-C2-1-P) and the Catalan Government GECA (2017 SGR 910). P.G-G (FPU AP2010-3596) and A.Z. (FPI BES-2014-070196) acknowledge their respective predoctoral scholarships.

## Literature Cited

Azam, F., and F. Malfatti. 2007. Microbial structuring of marine ecosystems. Nature Reviews Microbiology 5:782–791.

Biswas, J., Y. Liu, R. H. Singer, and B. Wu. 2019. Fluorescence imaging methods to investigate translation in single cells. Cold Spring Harbor Perspectives in Biology 11:a032722.

Borcard, D., F. Gillet, and P. Legendre. 2011. Numerical ecology with R. Springer, New York, New York, USA.

Buchaca, T., M. Felip, and J. Catalan. 2005. A comparison of HPLC pigment analyses and biovolume estimates of phytoplankton groups in an oligotrophic lake. Journal of Plankton Research 27:91–101.

Camarero, L., and J. Catalan. 2012. Atmospheric phosphorus deposition may cause lakes to revert from phosphorus limitation back to nitrogen limitation. Nature Communications 3:1118.

Camarero, L., M. Felip, M. Ventura, F. Bartumeus, and J. Catalan. 1999. The relative importance of the planktonic food web in the carbon cycle of an oligotrophic mountain lake in a poorly vegetated catchment (Redó, Pyrenees). Journal of Limnology 58:203–212.

Catalan, J. 1988. Physical properties of the environment relevant to the pelagic ecosystem of a deep high-mountain lake (Estany Redó, Central Pyrenees). Oecologia Aquatica 9:89–123.

Catalan, J., et al. 2006. High mountain lakes: extreme habitats and witnesses of environmental changes. Limnetica 64:123–145.

Catalan, J., M. Felip, P. Giménez-Grau, A. Zufiaurre, L. Camarero, and S. Pla-Rabés. 2020. Effects of episodic nutrients enrichments on P-limited planktonic communities - Lake Redon ENEX 2013 experiment. Dryad Dataset. https://doi.org/10.5061/dryad.tx95x69vh

Diaz, J., E. Ingall, C. Benitez-Nelson, D. Paterson, M. D. de Jonge, I. McNulty, and J. A. Brandes. 2008. Marine polyphosphate: a key player in geologic phosphorus sequestration. Science 320:652–655.

Droop, M. R. 1974. The nutrient status of algal cells in continuous culture. Journal of the Marine Biological Association of the United Kingdom 54:825–855.

Elrifi, I. R., and D. H. Turpin. 1985. Steady-state luxury consumption and the concept of optimum nutrient ratios: a study with phosphate and nitrate limited *Selenastrum minutum* (Chlorophyta). Journal of Phycology 21:592–602.

Elser, J. J., T. Andersen, J. S. Baron, A.-K. Bergström, M. Jansson, M. Kyle, K. R. Nydick, L. Steger, and D. O. Hessen. 2009. Shifts in lake N: P stoichiometry and nutrient limitation driven by atmospheric nitrogen deposition. Science 326:835–837.

Elser, J. J., M. E. S. Bracken, E. E. Cleland, D. S. Gruner, W. S. Harpole, H. Hillebrand, J. T. Ngai, E. W. Seabloom, J. B. Shurin, and J. E. Smith. 2007. Global analysis of nitrogen and phosphorus limitation of primary producers in freshwater, marine and terrestrial ecosystems. Ecology Letters 10:1135–1142.

Elser, J. J., and D. K. Foster. 1998. N: P stoichiometry of sedimentation in lakes of the Canadian shield: relationships with seston and zooplankton elemental composition. Ecoscience 5:56–63.

Felip, M., F. Bartumeus, S. Halac, and J. Catalan. 1999. Microbial plankton assemblages, composition and biomass, during two ice-free periods in a deep high mountain lake (Estany Redó, Pyrenees). Journal of Limnology 58:193–202.

Flynn, K. J., J. A. Raven, T. A. V. Rees, Z. V. Finkel, A. Quigg, and J. Beardall. 2010. Is the growth rate hypothesis applicable to microalgae? Journal of Phycology 46:1–12.

Fu, F.-X., Y. Zhang, K. Leblanc, S. A. Sañudo-Wilhelmy, and D. A. Hutchins. 2005. The biological and biogeochemical consequences of phosphate scavenging onto phytoplankton cell surfaces. Limnology and Oceanography 50:1459–1472.

Geider, R. J., and J. La Roche. 2002. Redfield revisited: variability of C:N: P in marine microalgae and its biochemical basis. Journal of Phycology 37:1–17.

Goldman, J. C., J. J. McCarthy, and D. G. Peavey. 1979. Growth rate influence on the chemical composition of phytoplankton in oceanic waters. Nature 279:210–215.

Grasshoff, K., M. Ehrhardt, and K. Kremling. 1983. Methods of seawater analysis. Second edition. Verlag Chemie, Weinheim, Germany.

Hall, S. R., V. H. Smith, D. A. Lytle, and M. A. Leibold. 2005. Constraints on primary producer N: P stoichiometry along N: P supply ratio gradients. Ecology 86:1894–1904.

Hessen, D. O., J. J. Elser, R. W. Sterner, and J. Urabe. 2013. Ecological stoichiometry: an elementary approach using basic principles. Limnology and Oceanography 58:2219–2236.

Hillebrand, H., C.-D. Dürselen, D. Kirschtel, U. Pollingher, and T. Zohary. 1999. Biovolume calculation for pelagic and benthic microalgae. Journal of Phycology 35:403–424.

Hillebrand, H., G. Steinert, M. Boersma, A. Malzahn, C. L. Meunier, C. Plum, and R. Ptacnik. 2013. Goldman revisited: Faster-growing phytoplankton has lower N : P and lower stoichiometric flexibility. Limnology and Oceanography 58:2076–2088.

Klausmeier, C. A., E. Litchman, T. Daufresne, and S. A. Levin. 2004*a*. Optimal nitrogen-to-phosphorus stoichiometry of phytoplankton. Nature 429:171–174.

Klausmeier, C. A., E. Litchman, F. Drive, and S. A. Levin. 2004*b*. Phytoplankton growth and stoichiometry under multiple nutrient limitation. Limnology and Oceanography 49:1463–1470.

Legendre, P., and E. D. Gallagher. 2001. Ecologically meaningful transformations for ordination of species data. Oecologia 129:271–280.

Loladze, I., and J. J. Elser. 2011. The origins of the Redfield nitrogen-to-phosphorus ratio are in a homeostatic protein-to-rRNA ratio. Ecology Letters 14:244–250.

Mahowald, N., et al. 2008. Global distribution of atmospheric phosphorus sources, concentrations and deposition rates, and anthropogenic impacts. Global Biogeochemical Cycles 22:1–19.

Martiny, A. C., C. T. A. Pham, F. W. Primeau, J. A. Vrugt, J. K. Moore, S. A. Levin, and M. W. Lomas. 2013. Strong latitudinal patterns in the elemental ratios of marine plankton and organic matter. Nature Geoscience 6:279–283.

Medina-Sánchez, J. M., M. Felip, and E. O. Casamayor. 2005. Catalyzed reported deposition-fluorescence in situ hybridization protocol to evaluate phagotrophy in mixotrophic protists. Applied and Environmental Microbiology 71:7321–7326.

Menden-Deuer, S., and E. J. Lessard. 2000. Carbon to volume relationships for dinoflagellates, diatoms, and other protist plankton. Limnology and Oceanography 45:569–579.

Moore, C. M., et al. 2013. Processes and patterns of oceanic nutrient limitation. Nature Geoscience 6:701–710.

Moreno, A. R., and A. C. Martiny. 2018. Ecological stoichiometry of ocean plankton. Annual Review of Marine Science 10:43–69.

Mullin, M. M., P. R. Sloan, and R. W. Eppley. 1966. Relationship between carbon content, cell volume, and area in phytoplankton. Limnology and Oceanography 11:307–311.

Murphy, J., and J. P. Riley. 1962. A modified single solution method for the determination of phosphate in natural waters. Analytica Chimica Acta 27:31–36.

Norland, S. 1993. The relationship between biomass and volume of bacteria. Pages 303–307 *in* P. F. Kemp, B. F. Sherr, E. B. Sherr, and J. J. Cole, editors. Handbook of methods in aquatic microbial ecology. Lewis Publishers, Boca Raton, Florida, USA.

Oksanen, J., F. G. Blanchet, R. Kindt, P. Legendre, P. R. Minchin, R. B. O'Hara, G. L. Simpson, P. Solymos, M. H. H. Stevens, and H. Wagner. 2016. Community ecology package "vegan". R Foundation for Statistical Computing, Vienna, Austria.

Peñuelas, J., et al. 2013. Human-induced nitrogen-phosphorus imbalances alter natural and managed ecosystems across the globe. Nature Communications 4:2934.

Persson, J., P. Fink, A. Goto, J. M. Hood, J. Jonas, and S. Kato. 2010. To be or not to be what you eat: regulation of stoichiometric homeostasis among autotrophs and heterotrophs. Oikos 119:741–751.

Quigg, A., Z. V. Finkel, A. J. Irwin, Y. Rosenthal, T.-Y. Ho, J. R. Reinfelder, O. M. Schofield, F. M. M. Morel, and P. G. Falkowski. 2003. The evolutionary inheritance of elemental stoichiometry in marine phytoplankton. Nature 425:291–294.

Redfield, A. C. 1963. The influence of organisms on the composition of sea-water. Pages 26–77 *in* M. N. Hill, editor. The Sea. Wiley Interscience, New York, New York, USA.

Rhee, G.-Y. 1978. Effects of N: P atomic ratios and nitrate limitation on algal growth, cell composition, and nitrate uptake. Limnology and Oceanography 23:10–25.

Sañudo-Wilhelmy, S. A., A. Tovar-Sanchez, F.-X. Fu, D. G. Capone, E. J. Carpenter, and D. A. Hutchins. 2004. The impact of surface-adsorbed phosphorus on phytoplankton Redfield stoichiometry. Nature 432:897–901.

Sournia, A. E. 1978. Phytoplankton manual. UNESCO, Paris, France.

Sterner, R. W., T. Andersen, J. J. Elser, D. O. Hessen, J. M. Hood, E. McCauley, and J. Urabe. 2008. Scale-dependent carbon:nitrogen:phosphorus seston stoichiometry in marine and freshwaters. Limnology and Oceanography 53:1169–1180.

Sterner, R. W., and J. J. Elser. 2002. Ecological stoichiometry: the biology of elements from molecules to the biosphere. Princeton University Press, Princeton, New Jersey, USA.

Van Mooy, B. A. S., et al. 2009. Phytoplankton in the ocean use non-phosphorus lipids in response to phosphorus scarcity. Nature 458:69–72.

Ventura, M., L. Camarero, T. Buchaca, F. Bartumeus, D. M. Livingstone, and J. Catalan. 2000. The main feature of seasonal variability in the external forcing and dynamics of a deep mountain lake (Redo, Pyrenees). Journal of Limnology 59:97–108.

Ventura, M., and J. Catalan. 2005. Reproduction as one of the main causes of temporal variability in the elemental composition of zooplankton. Limnology and Oceanography 50:2043–2056.

Wang, R., Y. Balkanski, O. Boucher, P. Ciais, J. Peñuelas, and S. Tao. 2014. Significant contribution of combustion-related emissions to the atmospheric phosphorus budget. Nature Geoscience 8:48–54.

Warner, K. A., J. E. Saros, and K. S. Simon. 2017. Nitrogen subsidies in glacial meltwater: implications for high elevation aquatic chains. Water Resources Research 53:9791–9806.

Weber, T. S., and C. Deutsch. 2010. Ocean nutrient ratios governed by plankton biogeography. Nature 467:550–554.

## Supporting Information

Additional Supporting Information may be found online at: http://onlinelibrary.wiley.com/doi/10.1002/ecs2.3249/full